ARPN Journal of Engineering and Applied Sciences

FABRICATION OF A THYROID PHANTOM FOR IMAGE QUALITY IN NUCLEAR MEDICINE USING THE 3D PRINTING TECHNOLOGY

Moayyad Alssabbagh[1], AbdulAziz Tajuddin[2], Mahayuddin Abdul Manap[1] and Rafidah Zainon[1]
[1]Advanced Medical and Dental Institute, Universiti Sains Malaysia, Bertam, Kepala Batas, Pulau Pinang, Malaysia
[2]School of Physics, Universiti Sains Malaysia, Pulau Pinang, Malaysia
E-Mail: sabmomo75@gmail.com

ABSTRACT

The attenuation values polycarbonate material was evaluated using the XCom database. The results were compared with the attenuation values of the human thyroid published by the International Commission on Radiation Units and Measurements - ICRU no. 44. The adult thyroid was designed from scratch as a 3D thyroid model using the 3Ds Max software. The model was then 3D printed with a Pursa i3 printer using the polycarbonate material. The Scintigraphy images were obtained after injection of Tc-99 inside the thyroid phantom. The results show that the polycarbonate material can be used as a tissue-equivalent substitute of human thyroid. The quality of the images in nuclear medicine was evaluated, where the images are similar to the images of a healthy human thyroid. The 3D printing technology shortens the time of phantom fabrication, and it shows good results to mimic the real geometry of the human thyroid.

Keywords: thyroid, phantom, 3D printing, mass attenuation coefficients.

INTRODUCTION

Gaining attention in the late 1990s, the 3D printing innovation technology is utilized generally these days as a part of numerous enterprises. The 3D printer utilizes an arrangement of three-dimensional images or any 3D attracting programming tests to develop the fancied three-dimensional model which is layered by the 3D printing material [1].

There are assortments of common 3D printing materials which are financially accessible. One of the most widely recognized and favored is Polycarbonate (PC). This type of 3D material is extremely tough and durable thermoplastic material that is used when making bulletproof glass. It is also temperature resistant that could reach up to 315 ^{o}C, and has a great layer to layer bonding, which provides an excellent finish when printed [2], [3].

Additionally, this material is malleable while cold and can be bent without cracking, has chemical resistance, toughness. It also has good physical properties and involved in many applications, such as 3D printer components subjected to heat and load, plastic lenses for eyeglasses, brackets and structural parts, exterior automotive components, equipment housings, outdoor lighting fixtures [4].

Commercial 3D printers are presently much more available, and they are not as expensive due to the competitive market. The RepRap machine is a popular 3D printer with an open-source venture that was built by a global volunteer community. As such, its viral circulation over the internet has resulted in the increasing manufacture of more than several thousands of machines worldwide[5].

3D printing technology in the medical field is now widespread. Anatomical structures can be printed from 3D images using computed tomography (CT) and magnetic resonance imaging (MRI) scanners to meet the accurate organ geometry. Likewise, this technology is now used on living cells to replace human body organs or parts, such as blood vessels, bones and ears for a short period. It is also utilized in the pharmaceutical industry to test new drugs [6].

Recently, many researchers have published their work on organ-mimicking phantom fabrication using 3D printing technology. A compelling study done by Cloonan et al. (2014) constructed a 3D human aorta using tissue substitute materials. The production of such phantoms using 3D printing technology and their mechanical properties was investigated. From this study, medical imaging and computational analysis improvements from experimental and clinical procedures were concluded (Cloonan*et al.*, 2014).

On the other hand, Cunha *et al.* (2015) evaluated the radiation attenuation attributes of the Polycarbonate (PC-ISO) 3D printing material that was to be used in brachytherapy. In his study, 3D printing technology was used to make a tailored, single-use of Gynecologic (GYN) brachytherapy applicators [7].

Generally, most of the phantoms today have basic geometric forms. Anthropomorphic thyroid phantoms of all sorts were made for different applications. Among these are thyroid-uptake phantoms that were made for tool calibration studies [8] and the thyroid phantom for counting the efficiency of the iodine isotope I-131 [9]. There are also the thyroid phantoms for quality control tests for healthy and disordered thyroids [10], as well as the neck phantom with thyroid inserts for medical dosimetry [11]. Nevertheless, such phantoms lack the preciseshape and sizes of the thyroid gland. In fact, changing the thyroid dimensions according to age and gender is not as simple. It is also unfortunate that fabricating these phantoms is time-consuming.

All in all, the present research has had polycarbonate evaluated in order to mimic the human thyroid gland. An original three-dimensional thyroid phantom was designed from scratch. Apparently, at least 95% of the real human thyroid can be simulated. Additionally, the accommodation of different gender and

ARPN Journal of Engineering and Applied Sciences

age categories is possible through the 3D printing technology for image quality purposes.

MATERIALS AND METHODS

3D printing polycarbonate material (Dong Guan Pioneer Trading CO, LTD, Dongguan, CN) was evaluated in this study. The elemental composition of a 3D printed sample of a polycarbonate with a size of 1 $cm^3$was attained by scanning the electron microscopy utilized in the Energy Dispersive X-ray Spectroscopy (SEM-EDS) machine (Quanta FEG 650; FEI, Hillsboro, OR, USA). Thence, the mass attenuation coefficient was calculated using the results obtained. This was done by using the XCOM photon cross-section database software[12] covering an energy range of 30 – 400 keV, where most radioisotopes used in nuclear medicine fall within this range.

The results of the polycarbonate material from XCOM were compared with the attenuation values of the thyroid from its elemental composition that is listed in the International Commission on Radiation Units and Measurements – ICRU, report no. 44.

The average diameter of 10 cm and 1 cm of neck phantom and trachea phantom for a paediatric patient of 10 years old were idealised[14]-[17]. The neck and trachea phantoms are both made of Polymethylmethacrylate (PMMA) material.

Literature, CT and Ultrasound images of real healthy thyroid gland used fordetermining the sizes and dimensions for the development of an adult thyroid gland, where the average length and width of each lobe for adults are about 3.5 cm and 2 cm respectively [18]. In other references, the average lobe size is 5cm in length, 2.5 cm in width and 1.5cm in depth [19].

This was done from scratch, where the 3Ds Max v.2013 software (Autodesk, San Rafael, CA) was used. A hollow-inside thyroid gland model was constructed for injecting radioactive materials for image quality evaluation in nuclear medicine as shown in Figure-1.

The design can be altered without difficulty to suit the various thyroid dimensions in all age groups. The phantom also has two holes on the top for injecting the radioactive material.

CURA ver. 2.1.0 (Ultimaker B.V., Geldermalsen, NL) was used to print out the STL file that converted from the 3Ds max software on Prusa i3. It is a 3D printer designed by Josef Prusa[20] and built by Lin Kuan Yang in Taiwan. The 3D printer made an accumulating method to accumulate the 3D material which was melted by an extruder. The resolution of the printer for each accumulated layer is 20 micrometers for the XY position and 5 micrometers for the Z position.

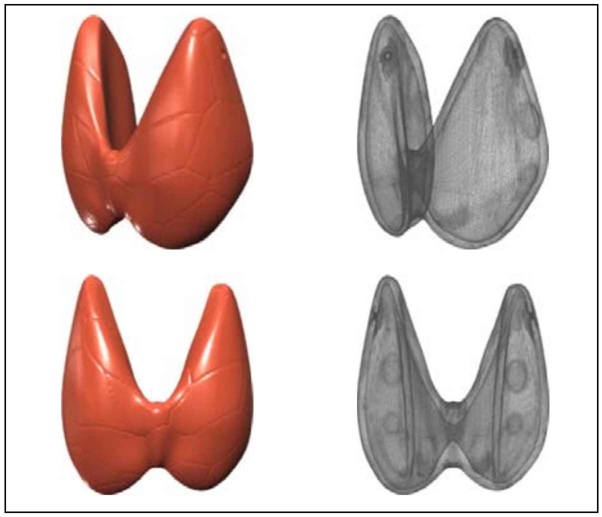

Figure-1. The designed 3D thyroid model.

The time taken to print out the paediatric thyroid phantom was roughly 10 minutes, whilst the expected time to print the adult size of the same model was expected to be about 20 minutes.

Table-1. The elemental compositions of polycarbonate and the thyroid gland.

	Elemental composition (% by mass)										
Elements	*** H**	**C**	**N**	**O**	**Na**	**P**	**S**	**Cl**	**K**	**I**	**Ti**
Polycarbonate	-	76.4	5.3	22.8	-	-	0.11	-	-	-	0.8
Thyroid *	10.4	11.9	2.4	74.5	0.2	0.1	0.1	0.2	0.1	0.1	-

* ICRU 44 [20]

ARPN Journal of Engineering and Applied Sciences

www.arpnjournals.com

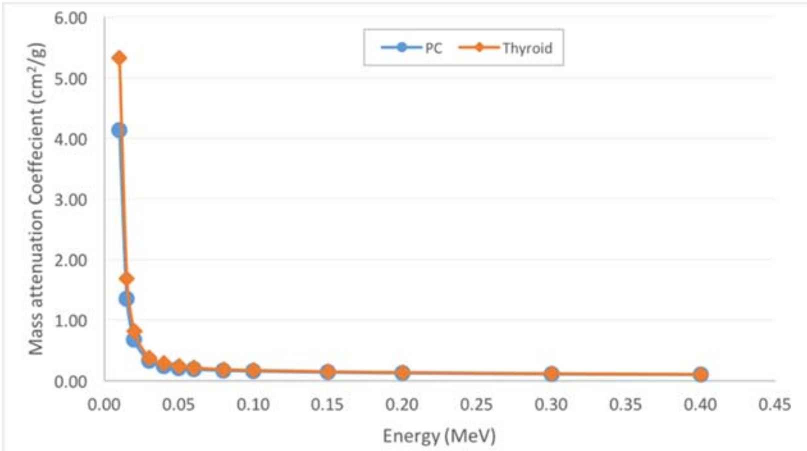

Figure-2. The mass attenuation coefficient of PC material compared with the human thyroid

RESULTS AND DISCUSSIONS

The elemental compositions of polycarbonate material from the SEM-EDS machine as well as the elemental composition of the thyroid gland as listed in ICRU-44 are displayed in Table-1. The results were employed as a contribution to the XCOM database to compute the mass attenuation coefficient for the polycarbonate material and the thyroid gland. To calculate the mass attenuation coefficients, an energy range for the nuclear medicine was applied.

As illustrated in Figure-2, the mass attenuation coefficients of the polycarbonate and thyroid show a match. The total mass attenuation coefficient of the polycarbonate was divided by the total attenuation values of the thyroid to acquire the ratio between them. The mean ratio and the standard deviation of the polycarbonate and thyroid were 0.9 ± 0.03, which is very close to 1. The ratio that has the nearest value to 1 was acknowledged as an appropriate material choice. No significant variances were revealed among the attenuation values of the EDS machine and the chemical formula for polycarbonate.

The 3D printed thyroid was effectively made with the Prusa i3 3D printer (Figure-3).

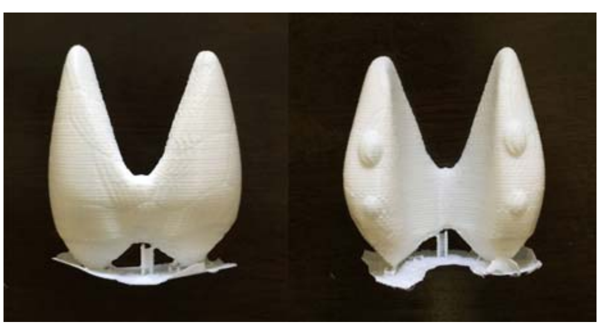

Figure-3. The fabricated 3D paediatric thyroid.

Prior to print production, the dimensions can be altered between adult and child thyroid sizes using the CURA software. Since females and males have somewhat dissimilar thyroid lobe sizes, the dimension of each lobe can be altered conferring to the target age and gender via the same software. Figure 4 illustrates this concept. A minimal of 90% to 95% of the actual shape and size of a human thyroid gland can be simulated with the 3D fabricated model. This comes with changeable geometrical shape-size features to suit all ages.

Figure-4. The 3D printed thyroid with different sizes using the Cura software.

For phantom evaluation, the radioisotope Technetium (TC-99m) was injected in the 3D thyroid phantom. SPECT-CT with a dual head gamma camera (GE Healthcare, Waukesha, WI) was used to get the thyroid scintigraphy images to assess the image quality formed in nuclear medicine. Figure-5 displays the size and shape of the 3D thyroid phantom as being similar to normal thyroids in good physical shape. This means the radioisotope is distributed uniformly in the fabricated phantom. The imaging system will be assessed using a suitably acquired image of the phantom.

ARPN Journal of Engineering and Applied Sciences

www.arpnjournals.com

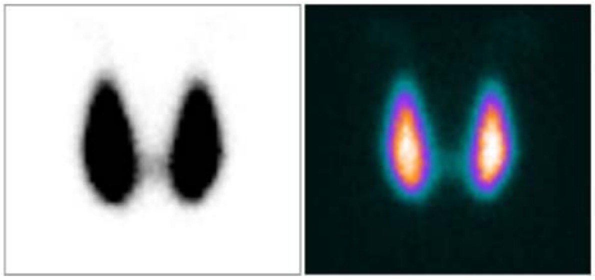

Figure-5. The Scintigraphy image of the 3D thyroid phantom.

CONCLUSIONS

Polycarbonate (PC) material was found to have a good match with the human thyroid in terms of its elemental compositions and mass attenuation coefficients. The attenuation properties of the PC material presented a very good match with the thyroid tissue when the energy is increased. This allows it to be used at high applied voltages in radiotherapy. A novel model of the thyroid was indigenous, which simulates a minimum 95% of the actual shape and size of a human thyroid.

Additionally, the dimensions of the designed model can be modified prior to printing, to simulate paediatric and adult thyroids, each for both genders. The phantom has a hollow-inside structure to be used in nuclear medicine. The images from the nuclear medicine show that the phantom can be used for image quality evaluation, where the radioactive material distributed uniformly inside the phantom.

The time needed to print out the 3D thyroid phantom was reduced to an average period of 10 minutes compared to the conventional method that is lengthier. Lastly, the 3D printing material in this research is cost-effective and available commercially in comparison with present saleable tissue-equivalent materials.

For future work, this hollow-inside model of thyroid could be filled with water, which is a soft tissue equivalent, and accommodate dosimeters, such as TLD to be used in both nuclear medicine and diagnostic X-ray fields for dosimetry and image quality research.

REFERENCES

[1] 3ders. 2016. What is 3D Printing? [Online]. Available: http://www.3ders.org/3d-printing.html. [Accessed: 15-Dec-2016].

[2] T. Koslow. 2015. Polymaker and Bayer Team for Desktop Polycarbonate 3D Printing Filaments. [Online]. Available: https://3dprintingindustry.com/news/polymaker-bayer-team-for-desktop-polycarbonate-3d-printing-filaments-57619/.

[3] MatterHackers. 2015. 3D Printer Filament Comparison. MatterHackers. [Online]. Available: https://www.matterhackers.com/3d-printer-filament-compare.

[4] Airwolf3D. 2005. Why Polycarbonate Filament?[Online]. Available: http://airwolf3d.com/shop/polycarbonate-filament-2-88mm-2-and-5lbs.

[5] A. Bowyer. 2014. 3D Printing and Humanity's First Imperfect Replicator. 3D Print. 1(1): 2013-2014.

[6] C. Schubert, M. C. van Langeveld, and L. A. Donoso. 2014. Innovations in 3D printing: a 3D overview from optics to organs. Br. J. Ophthalmol. 98(2): 159-61.

[7] J. A. M. Cunha *et al.* 2015. Evaluation of PC-ISO for customized, 3D Printed, gynecologic 192-Ir HDR brachytherapy applicators. J. Appl. Clin. Med. Phys. 16(1): 5168.

[8] Marshall Brucer. 1959. Thyroid Radioiodine Uptake Measurement: A Standard System for Universal Intercalibration. Oak Ridge Inst. Nucl. Stud. ORINS.No. 19.

[9] G. H. Kramer, K. Gamarnik, L. Noel, L. Burns, and D. Meyerhof. 1996. The BRMD Thyroid-Neck Phantom: Design and Construction. Health Phys. 71(2).

[10] R. A. D. Cerqueira and A. F. Maia. 2014. Development of thyroid anthropomorphic phantoms for use in nuclear medicine.Radiat. Phys. Chem. 95: 174-176.

[11] S. MehdizadehNaderi*et al.* 2016. Design and fabrication of a multipurpose thyroid phantom for medical dosimetry and calibration.Radiat. Prot. Dosim. 168(4): 503-508.

[12] Berger M J and Hubbell J H. 1987/. 1999. XCOM: Photon Cross Sections Database, Web Version 1.2. Natl. Inst. Stand. Technol. Gaithersburg, MD 20899, USA. Orig. Publ. as NBSIR 87-3597 "XCOM Phot. Cross Sect. a Pers. Comput.

[13] S. L. Katz, J.-P. Vaccani, J. Clarke, L. Hoey, R. C. Colley and N. J. Barrowman. 2014. Creation of a reference dataset of neck sizes in children: standardizing a potential new tool for prediction of obesity-associated diseases? BMC Pediatr. 14(1): 159.

[14] D. Wheeler, J. Spaeth, R. Mehta, S. Hariprakash, and P. Cox. 2009. Assessment and Management of the Pediatric Airway. in Resuscitation and Stabilization of

the Critically Ill Child SE - 4, D. S. Wheeler, H. R. Wong, and T. P. Shanley, Eds. Springer London. pp. 1-30.

[15] N. T. Griscom and M. E. B. Wohl. 1986. Dimensions of the growing trachea related to age and gender. Am. J. Roentgenol. 146(2): 233-237.

[16] ICRP 89. 2002. Basic anatomical and physiological data for use in radiological protection: reference values. in Annals of the ICRP. J. Valentin, Ed. 32(3-4): 1-277.

[17] L. Wartofsky and D. Van Nostrand. 2007. Thyroid Cancer: A Comprehensive Guide to Clinical Management. Humana Press.

[18] I. R. McDougall. 200. Thyroid Cancer in Clinical Practice. Springer London.

[19] Prusa Josef. 2016. Prusa i3 3D Printer. [Online]. Available: http://reprap.org/wiki/Prusa_i3. [Accessed: 15December 2016].

[20] ICRU. 1989. Tissue Substitutes in Radiation Dosimetry and Measurement. ICRU Report 44.